

# **Solomon Curve 2020: Relating Microscopic Risk Models to Accident Statistics**

**Julian Eggert**

**2016**

**Preprint:**

This is an accepted article published in Intelligent Transportation Systems Conference (ITSC) 2016. The final authenticated version is available online at: [https://doi.org/\[DOI not available\]](https://doi.org/[DOI not available])

# Solomon Curve 2020: Relating Microscopic Risk Models with Accident Statistics

Julian Eggert<sup>1</sup>

**Abstract**—Traffic accident statistics as functions of the involved accident parameters are important sources of information to investigate accident causes. However, since traffic accidents are sparse events and the factors that lead to an accident can be very diverse, it is difficult to establish a direct link which relates microscopic risk models to the empirical findings. One seminal and widely debated work on accident statistics on multi-lane roadways is given by the so-called “Solomon curve” [1], which describes the collision rate of automobiles as a function of their speed. While one particular characteristic of the Solomon curve - its u-shape - has been explained theoretically in terms of traffic flow of passing cars in [2], a detailed derivation from microscopic risk models is still missing. In this paper, we start from a first-principles generalized risk model, and reconfirm the explanation of the curve, revealing that its parameters can be fully mapped to the parameters of the underlying microscopic risk model. In addition, an unexplained effect of the Solomon curve - the asymmetry of its minimum with respect to the average velocity - is predicted and explained by the derivation. The result then is two-fold: On one hand, we can now fully understand the Solomon curve in terms of microscopic risk parameters, and on the other hand, the empirical findings of the Solomon curve serve as a validation of the risk model and can be used to gain reasonable settings for microscopic risk parameters.

## I. INTRODUCTION

One important target of road and traffic development agencies, insurance companies as well as motor vehicle manufacturers is the reduction of the quantity and severity of traffic accidents. For this purpose, both regulatory affairs and vehicle construction strategies require a detailed empirical assessment of the complex interactions that vehicle, roadway, and human factors have on resulting accidents. Extensive statistical analyses have been conducted over the last decades to determine the different involved risk factors, as well as the injury levels and the crash frequency. With the advent of sensor-equipped vehicles and corresponding fleet tests (see e.g. [3]), data is accumulating at an exponential pace, so that it is expected that insight into this matter will also increase faster than before.

A large portion of the studies concentrate on human factors like driver distraction and inattention, fatigue-, drug-, alcohol-, gender- and age-related effects, as well as talking, texting or using devices during driving or driving in haste (see e.g. [4], [5]). Many of these factors have a modulating effect on the accident likelihood, so that e.g. a certain degree of distraction causes a late reaction, loss of control and finally leads to an accident. However, many other physical factors

related to the driving context (like traffic density, ego-vehicle speed and proximity to another vehicle) have an influence on the current accident risk that is at least as important. The problem here is the mere quantity of influential variables, from which usually several are not observable or unknown for the statistical analysis. In addition, it is usually hard to dissect which of the many factors are the most influential ones.

For microscopic risk models, the target is opposite: Starting from the current observations of the driving context as well as the driver state, based e.g. on information from external and internal sensors, we want to estimate the risk that a dangerous event like an accident can happen within a future time interval. This capability is a prerequisite for future Advanced Driver Assistance Systems (ADAS) and Autonomous Driving (AD) functions, since it builds the basis for schemes for behavior evaluation and planning based on risk minimization. It has been shown that microscopic risk models can be used successfully to describe and reproduce complex driving behaviors involving lane-changes, overtaking, intersection and entrance timing problems, and more, see e.g. [6], [7], [8], [9]. One pressing problem for risk models is their proper parameterization, which often is done by heuristics and rules-of-thumb derived from driving experience, like the fact that a certain minimal distance gap should be kept during car following. A grounded validation of the involved parameters would be desirable here.

In this paper, we investigate the relationship between large-scale statistics of collision rates on rural highways presented first in [1] with a probabilistic, microscopic risk model of collision accident events based on a distance-based risk as presented in [6]. We find that the empirically measured accident vs. speed curves can be derived using the microscopic risk model, confirming an early suggestion of Hauer ([2]) that differential speed and passing is the main cause of accidents in that context. Moreover, our derivation provides an explanation of a controversially disputed asymmetry which was observed in the measurements. In addition, the mapping between the microscopic risk model and the accident statistics allows an empirical validation of the risk model parameters.

## II. THE SOLOMON CURVE

A large number of factors contribute to the risk of traffic incidents, comprising vehicle and infrastructure conditions such as vehicle setup, road design, road infrastructure on one side, human (driver) factors like driver skills, impairment, alertness, risk and speeding propensity as well as general

<sup>1</sup>Julian Eggert is with the Honda Research Institute (HRI) Europe, Carl-Legien-Str. 30, 63073 Offenbach, Germany  
julian.eggert@honda-ri.de

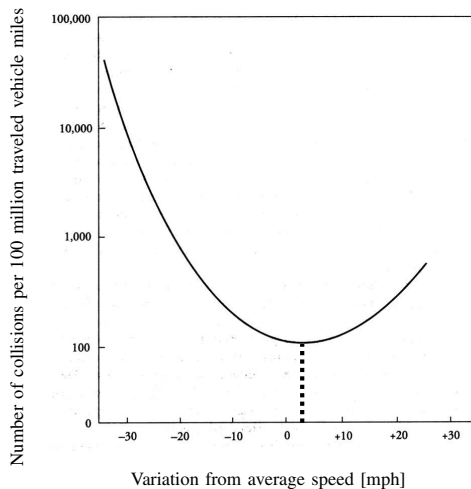


Fig. 1. The U-shaped Solomon curve, after [1] (image free of copyright), at logarithmic scale. Number of collisions as a function of speed. The collision risk increases for travelling speeds **both faster and slower** than average speed, and exhibits a minimum slightly higher than average speed.

behavior on the other side, and last but not least the specific driving situation including traffic density, visibility, weather conditions and the velocities, distances and behaviors of neighbouring traffic participants before a critical incident.

Studies which try to relate these factors to traffic accident statistics therefore usually reveal multiple causes, which complicates a microscopic modeling in term of risk factors. That is one reason why the analysis conducted by David Solomon in the late 1950's [1] caught large attention. The work comprised a comprehensive study of more than 10000 collision cases and how road, driver and vehicle characteristics affect the probability of being involved in a crash. One result from the analysis, currently known as the **Solomon curve** or **Crash Risk Curve**, is a graphical representation of the average collision rates on rural highways as a function of speed, see fig. 1. In subsequent discussions and research, significant biases in the analysis have been revealed, casting doubt on details of Solomon's work (see e.g. [10]), however the general findings have been largely confirmed, see [11], [12], [13], [14], [15].

In detail, the Solomon curve takes experimentally determined accident involvement rates (number of accidents divided by the related vehicle miles of travel) and compares them to the driving speed. It exhibits a pronounced U-shape with a minimum that is roughly located around the average driving speed, see fig. 1 (by average driving speed we mean the mean operating speed in a road segment). The risk of having a crash is therefore increased both for vehicles traveling slower than the average speed, and for those traveling above the average speed. While the crash frequency increase for high absolute speeds seems understandable due to a higher chance that the driver loses control, the reasons for the increase at speeds lower than the average have been disputed, e.g. arguing a posteriori that the low-speed data

may be originated under bad road conditions or that low-speed driving might be correlated with old, unexperienced or hesitant drivers having poor driving records. Again, however, up to the present time there has been no evidence to alter Solomon's original findings. As a consequence, the general advice to drivers that can be drawn from the results is that the safest way is to drive with the traffic flow.

In 1971, Hauer [2] provided a theoretical foundation for the Solomon curve. He started from traffic flow equations to calculate how many cars will pass a reference car or how many cars a reference car will pass, and deriving from that the accident involvement rate. He showed that the resulting curve was also U-shaped around the median travel speed. Hauer's work suggests a cause-effect interpretation for the variation of the accident probability with speed which relies on the passing events only, without the need for further causal explanations. It basically states that from the statistics, the accident frequency can be directly correlated with the number of passing maneuvers, which seems reasonable when considering that it is in these situations that cars come closest to each other.

The U-shape of the Solomon curve shows that the greater the difference between a drivers speed and the average traffic speed (both above and below that average speed) the greater the likelihood of involvement in a crash, with a more than exponential increase to both sides. One particularly intriguing property is that it has a minimum not at the average speed but at slightly higher speeds (indicated in fig. 1), suggesting that it may be even safer to drive slightly faster than the majority of vehicles. The origin of this asymmetry is still unexplained.

After this introduction of the Solomon findings and its theoretical explanation by Hauer, we will reconsider the derivation of the curves from a generalized microscopic risk model. We will concentrate on spatial risk probability between pairs of cars as the main risk source, and then follow an argumentation similar to Hauer, concentrating on collision statistics in 2-car passing situations. We will show that the U-shaped curve can indeed be derived, with a few further extensions, from a first-principles risk-based approach, providing an explanation for the observed minimum asymmetry. At the same time, the theoretical derivation and its fit to the Solomon curve allows to find values for the contained microscopic risk parameters, and the subsequent generalization of the risk estimation towards arbitrary driving situations.

### III. A GENERALIZED MICROSCOPIC RISK MODEL

#### A. Survival Probabilities

Risk modeling involves two components: (i) the estimation of the occurrence frequency of critical events and (ii) the estimation of the severity in case that this critical event happens. This is a direct consequence from the definition of risk as the "probability of something happening multiplied by the resulting cost or benefit if it does" [16], [17]. The calculation of the severity is usually the straightforward case, modeling e.g. the physical crash for some given predicted

parameters at impact time like velocities and impact angle. The estimation of the occurrence frequency of a critical event implies the prediction of future states and is more difficult, mainly because of unknown data and uncertainties in this prediction, which require a probabilistic modeling approach.

The Solomon curve only deals with collision rates, so that in the following we disregard the severity (e.g. the fact that higher crashes at higher velocities tend to be more severe) and concentrate instead only on the collision probability.

The generalized risk model [6] quantifies accidents as a thresholding process based on a Poisson-like event probability. In this case, for a specific vehicle, in a sufficiently small time interval of size  $\Delta t$ , the so-called **instantaneous event probability** is characterized by an **event rate**  $\hat{\tau}^{-1}$ , so that

$$\hat{I}_{\text{event}}(\Delta t) := \hat{\tau}^{-1} \Delta t \quad . \quad (1)$$

The term instantaneous event probability denotes the fact that this probability does not take the history into account, so that it is assumed that no event has taken place before and at most 1 event will take place during the time interval.

The next important function is the **survival probability**  $\hat{S}(t+s;t)$ , which indicates the probability that, starting at  $t$ , a particular vehicle will survive for a certain amount of time  $s$  until  $t+s$ , i.e., that it will not be engaged in an event like e.g. an accident. From (1), we directly get the survival probability after an additional small time interval  $\Delta t$ , if the survival probability at  $t'$  was  $\hat{S}(t';t)$  ( $t' \geq t$ ),

$$\begin{aligned} \hat{S}(t' + \Delta t; t) &= \hat{S}(t'; t) \hat{I}_{\text{no events}}(\Delta t) \\ &= \hat{S}(t'; t) [1 - \hat{I}_{\text{event}}(\Delta t)] \\ &= \hat{S}(t'; t) [1 - \hat{\tau}^{-1} \Delta t] \end{aligned} \quad (2)$$

From this difference equation we then get first that  $[\hat{S}(t' + \Delta t; t) - \hat{S}(t'; t)]/\Delta t = \hat{S}(t'; t) \{-\hat{\tau}^{-1}\}$  and for arbitrarily small  $\Delta t \rightarrow 0$ , we arrive at  $\hat{S}(t' + s; t) = \hat{S}(t'; t) \exp\{-\hat{\tau}^{-1}s\}$  so that with the starting condition  $\hat{S}(t;t) = 1$  we get

$$\hat{S}(t+s;t) = \exp\{-\hat{\tau}^{-1}s\} \quad (3)$$

which describes the **homogeneous survival probability** (constant  $\hat{\tau}^{-1}$ ) between  $t$  and  $t+s$ , with a chance of surviving which decays exponentially from 1 at  $s=0$  to 0 for  $s=\infty$ .

The real risk event modeling now occurs by a proper parameterization and variation of the time-varying  $\hat{\tau}^{-1}(t)$  resp. its state-dependent analogous function  $\tau^{-1}(\mathbf{z}_t)$ , with  $\hat{\tau}^{-1}(t) = \tau^{-1}(\mathbf{z}_t)$ . In  $\tau^{-1}(\mathbf{z}_t)$ , we include all the risk factors, i.e., the context information and eventually the human state in a state vector  $\mathbf{z}$ . Correspondingly, for dangerous situations, the event rate will be higher than for harmless situations.

Now let us assume that we split the interval of length  $s$  into several subintervals of length  $\Delta t$ , where for each interval  $\hat{\tau}^{-1}(t)$  is constant, then we get

$$\hat{S}(t+s;t) = e^{\{-\hat{\tau}^{-1}(t)\Delta t\}} e^{\{-\hat{\tau}^{-1}(t+\Delta t)\Delta t\}} \dots \quad (4)$$

(i.e., a vehicle survives from  $t$  to  $t+s$  if it first survives the sub-interval from  $t$  to  $t+\Delta t$  and then from  $t+\Delta t$  to  $t+2\Delta t$  and so on until  $s$ ). With  $\Delta t \rightarrow 0$  we then arrive at the

**inhomogeneous survival probability** (temporally varying  $\hat{\tau}^{-1}(t)$ )

$$\hat{S}(t+s;t) = \exp\left\{-\int_0^s \hat{\tau}^{-1}(t+s') ds'\right\} \quad . \quad (5)$$

The states have been left out here for simplicity of the derivations. If we include them back we get the state-dependent survival probability function

$$S(t+s;t, \mathbf{z}_{t:t+s}) = \exp\left\{-\int_0^s \tau^{-1}(\mathbf{z}_{t+s'}) ds'\right\} \quad (6)$$

which defines the probability that a vehicle survives during  $[t, t+s]$  without being involved in a critical event and which depends on the entire state vector sequence  $\mathbf{z}_{t:t+s}$ . Similarly, the state-dependent instantaneous event probability then is

$$I_{\text{event}}(\Delta t, \mathbf{z}_t) := \tau^{-1}(\mathbf{z}_t) \Delta t \quad . \quad (7)$$

### B. Instantaneous Event Rates and Spatial Risk

In the following, we will concentrate on the most important context information for collision accidents: the spatial proximity between traffic participants. In the following, we consider the ego car within a set of  $N$  other cars, with the ego-vehicle position  $\mathbf{x}^o$ , another vehicle  $i > 0$  position  $\mathbf{x}^i$  and the spatial distance between the ego vehicle and another car  $d^{o,i}$ . In this case, we have

$$\mathbf{z} := \{\mathbf{x}^o, \mathbf{x}^i\} \text{ with } d^{o,i}(\mathbf{z}) = \|\mathbf{x}^o - \mathbf{x}^i\| \quad (8)$$

and

$$D^{o,i}(\mathbf{z}) := \min\{0, [d^{o,i}(\mathbf{z}) - d_{c,min}]\} \quad (9)$$

We then model, for quantifying the risk of an accident between the ego-car and each other car, the (time-varying!) spatial risk collision event rate  $\tau_c^{-1}(\mathbf{z})$  by

$$\tau_c^{-1}(\mathbf{z}) = \tau_{c,o}^{-1} e^{-\beta_c D^{o,i}(\mathbf{z})} \quad (10)$$

with constants  $\tau_{c,o}^{-1}$ ,  $\beta_c$  and  $d_{c,min}$  chosen so that the instantaneous event probability contribution of each other car approaches 1 when the distance reaches a certain minimal contact distance  $d_{c,min}$  which implies a physical collision (for car-to-car collisions,  $d_{c,min}$  is therefore usually chosen to be around 4 m). The steepness factor  $\beta_c$  is used to model uncertainties involved in the risk estimation, originated from several possible sources like sensor inaccuracy, state prediction errors, unexpected driver behavior or unknown vehicle sizes, which all lead to a misestimation of the distance and therefore to a possible accident even if the measured distance  $d^{o,i}$  is still larger than  $d_{c,min}$ .

For vehicles on roads, it is beneficial to model the spatial risk event rate separately for longitudinal and lateral distance components. Similarly to (9), for each other vehicle we then have longitudinal and lateral distances based on longitudinal and lateral coordinates  $x_{c,lon}^i$  and  $x_{c,lat}^i$ , respectively,

$$\begin{aligned} D_{lat}^{o,i}(\mathbf{z}) &:= \min\{0, [|x_{lat}^o - x_{lat}^i| - d_{c,lat,min}]\} \\ D_{lon}^{o,i}(\mathbf{z}) &:= \min\{0, [|x_{lon}^o - x_{lon}^i| - d_{c,lon,min}]\} \end{aligned} \quad (11)$$

and an event rate

$$\tau_c^{-1}(\mathbf{z}) = \tau_{c,o}^{-1} e^{-\beta_{c,lat} D_{lat}^{o,i}(\mathbf{z})} e^{-\beta_{c,long} D_{lon}^{o,i}(\mathbf{z})} \quad . \quad (12)$$

Interesting to observe is the effect of the risk event rate  $\tau^{-1}(\mathbf{z})$  on the survival probability. Every time a high  $\tau^{-1}(\mathbf{z})$  is encountered, the survival probability decreases by a certain step, as can be seen in figure 2. This occurs at points in time where the two vehicles approach each other, leading to an increase of the instantaneous accident probability, and therefore, to a reduced probability of “surviving”. The steepness and depth of the survival probability decay depends on the steepness factor  $\beta_c$  of the event rate as well as on the relative velocity between the vehicles, because a lower velocity means a shorter time that the ego-car is subject to the collision risk. As a rule of thumb, in terms of collision event probability, it is favorable to keep the time periods exposed to a certain risk as short as possible, so that passing a risky zone fast is beneficial. We will return to this paradoxical effect later in our section VI.

However, an overall risk consideration is more complex, since higher speeds have other risk-related effects. On one side, severity increases for crashes at high velocities (more kinetic energy is involved), on the other side controllability is reduced so that small driving errors (e.g. small movements on the steering wheel) have larger effects, up to the point where there is a risk of total loss of control on the vehicle. Such further risks are modeled by using a composed event rate like

$$\tau^{-1}(\mathbf{z}) := \tau_c^{-1}(\mathbf{z}) + \tau_l^{-1}(\mathbf{z}) + \dots \quad (13)$$

which comprises terms related to vehicle-to-vehicle collisions, loss of control, etc.

### C. Accident Probabilities

Combining the findings from the previous section, in particular (6) and (7), the total **event probability** that an event occurs within a small time interval  $\Delta t$  after a time  $s$  has passed, can be calculated by combining the probability  $S(t+s; t)$  that the vehicle survives from  $t$  until  $t+s$ , multiplied by the probability that an event will happen in the interval of length  $\Delta t$  around  $t+s$ . This results in

$$E_{\text{event}}(t+s; t, \Delta t, \mathbf{z}_{t:t+s}) = I_{\text{event}}(\Delta t, \mathbf{z}_{t+s}) S(t+s; t, \mathbf{z}_{t:t+s}) \quad (14)$$

This is the probability that an event will happen in an interval  $[t+s, t+s+\Delta t]$ , given a state vector history  $\mathbf{z}_{t:t+s}$ , if we start observations at  $t$  and no event happened during  $[t, t+s]$ .

Correspondingly, the **event density** (i.e., the probability of events per time unit) after a time  $s$  starting at  $t$  is given by

$$e_{\text{event}}(t+s; t, \mathbf{z}_{t:t+s}) := E_{\text{event}}(t+s; t, \Delta t, \mathbf{z}_{t:t+s}) / \Delta t = \tau^{-1}(\mathbf{z}_{t+s}) S(t+s; t, \mathbf{z}_{t:t+s}) \quad (15)$$

Intuitively, a vehicle that ceases to survive must have been engaged in an event and vice-versa, and from taking the derivative of (6) it can indeed be verified that

$$e_{\text{event}}(t+s; t, \mathbf{z}_{t:t+s}) = -\frac{d}{ds} S(t+s; t, \mathbf{z}_{t:t+s}) \quad (16)$$

which we use for integrating (15), to calculate the accumulated probability that an event will happens during a time

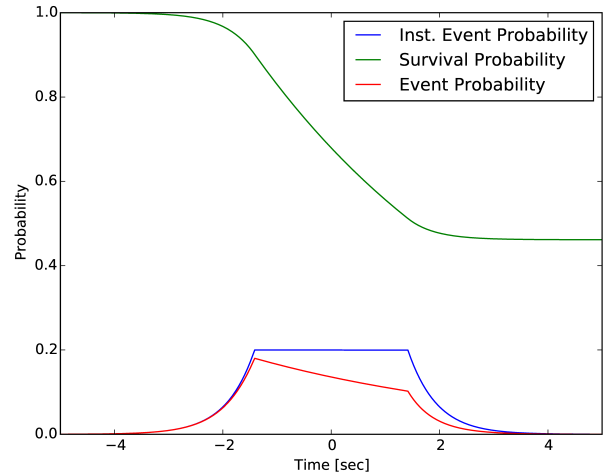


Fig. 2. Instantaneous event probability, event probability and survival probability as a function of elapsed time  $s$ . The **instantaneous event probability** (7) is memory-less and indicates the imminent level of criticality. The **survival probability** indicates the probability that a vehicle will remain safe (i.e., will survive) for a certain time span. The **event probability** indicates the probability that, after a certain time, a vehicle will be engaged in an event for the first time, i.e., if it survived until that time, and is a combination of the former two.

interval of length  $s$ , again starting at  $t$ . This then amounts to the survival probability difference,

$$A_{\text{event}}(t+s; t, \mathbf{z}_{t:t+s}) := \int_0^s e_{\text{event}}(t+s'; t, \mathbf{z}_{t:t+s'}) ds' = 1 - S(t+s; t, \mathbf{z}_{t:t+s}) \quad (17)$$

which is straightforward realizing that those vehicles which do not survive during  $[t, t+s]$  are exactly those that were engaged in an event during that time interval.

It is important to correctly distinguish the 3 introduced terms **instantaneous event probability**  $I_{\text{event}}(\Delta t, \mathbf{z}_t)$  (7), **survival probability**  $S(t+s; t, \mathbf{z}_{t:t+s})$  (6) and **event probability**  $E_{\text{event}}(t+s, t, \Delta t, \mathbf{z}_t)$  (14). Whereas  $I_{\text{event}}(\Delta t, \mathbf{z}_t)$  has no memory and only accounts for the current risk,  $E_{\text{event}}$  takes the history into account (with the help of the survival function), by observing the risk factors during a prolonged time interval of length  $s$ . Figure 2 shows the time course of the 3 factors for a distance-based risk and constant-velocity-difference passing situation between two cars (at  $s = 0$ , the cars come closest to each other). One can see that the instantaneous event probability increases with decreasing distance, symmetrically around  $s = 0$ . When the instantaneous event probability gets high, the survival probability starts to decrease, because there is a certain chance that an accident will happen. After passing each other the survival probability settles at a lower constant because in some occasions the cars will have been engaged in an accident event.

## IV. ACCIDENT PROBABILITY OF PASSING AND BEING PASSED

### A. Car Motion and Distance-Based Collision Event Rates

Eq. (17) is now our central ingredient for calculating the long-term collision accident frequencies. We start with modeling the trajectories  $\mathbf{x}_{t:t+s}^o$  and  $\mathbf{x}_{t:t+s}^i$  of the ego-vehicle

and the other vehicles. From this we get the distances (9) and calculate the distance-based risk event rates (10). Integration yields the survival function (6) and from this we get the accumulated probability of collision events (17).

In the following, we apply the generalized risk approach outlined in the previous section within a driving context characteristic for the Solomon-type research on collision frequencies. For this, we assume that

- each vehicle drives at a constant velocity  $v$ ,
- the vehicle velocities obey a known distribution  $p(v)$ ,
- frontal and backside approaches have the same propensity to lead to accidental events,
- the spatial traffic density  $\rho(x)$  is constant in the vicinity of the ego vehicle.

In the following, we write  $x$  instead of  $x_{c,lon}$  for simplicity. Without loss of generality, setting  $x^o = 0$  and  $t = 0$  as a starting point (we measure all positions relative to the starting point of the ego-vehicle), the ego-vehicle longitudinal position and velocity is then given by

$$x^o(s) = v^o s \quad (18)$$

and the other cars' ( $i > 0$ ) longitudinal position and velocity is

$$x^i(s) = x^i + v^i s \quad (19)$$

Comparing the ego-trajectory with the trajectory of another car, the crossing point resp. the time of closest encounter is then at  $s_c$  when  $x^o(s) = x^i(s)$ , or

$$s_c(v^o, x^i, v^i) = -\frac{x^i}{(v^i - v^o)} \quad (20)$$

Since we look from  $t = 0$  into the future  $s$ , it must be  $s_c(x, v) \geq 0$  and this can only be fulfilled under two conditions:

$$x^i \geq 0 \text{ and } v^i \leq v^o \quad (21)$$

(ego-car passes other car) or

$$x^i \leq 0 \text{ and } v^i \geq v^o \quad (22)$$

(ego-car is being passed by other car).

### B. Risk of Longitudinal Passing

For longitudinal passing maneuvers without lane change, the lateral distance  $D_{lat}^{o,i}$  from (11) remains constant, and using the car motion model from section (IV-A) for the longitudinal distances we get the collision event rate

$$\tau_c^{-1}(\mathbf{z}) = \overbrace{(\tau_{c,o}^{-1} e^{-\beta_{c,lat} D_{lat}^{o,i}})}^{:= \tilde{\tau}_{c,o}^{-1}} e^{-\beta_{c,lon} D_{lon}^{o,i}(\mathbf{z})} = \tilde{\tau}_{c,o}^{-1} e^{-\beta_{c,lon} D_{lon}^{o,i}(\mathbf{z})} \quad (23)$$

with the modified, new constant  $\tilde{\tau}_{c,o}^{-1}$  which comprises the lateral distance  $D_{lat}^{o,i}$ .

With this event rate, calculation of the ego-vehicle survival function according to (6) for 2-vehicle constant-velocity passing maneuvers results in a survival probability that exhibits a drop at the moment when the two cars pass each other. This can be seen in fig. (3), where we have set the

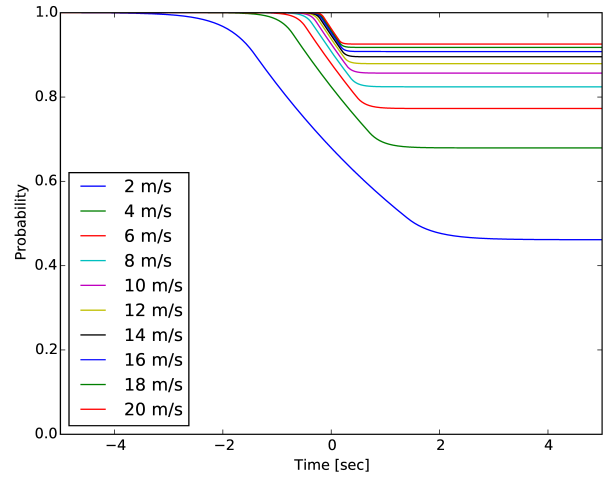


Fig. 3. Ego-vehicle survival probability for two vehicles passing each other as a function of time, plotted for different relative velocities and constant velocity assumptions. At the point of closest encounter (at  $s=0$  in the figure), the survival probability drops suddenly, because the distance-based risk increases. From this survival probability function, the overall accident frequency as a consequence of passing maneuvers is calculated.

conditions in a way that the two cars pass each other (point of closest approach) at  $s = 0$ . Around that point in time, the collision event rate (23) increases exponentially, leading to a higher instantaneous event probability and therefore to a pronounced decrease in the probability of survival. Before and after passing, the survival probability remains constant because the spatial risk vanishes for larger distances.

The slope of the survival probability drop during passing mainly depends on  $\beta_{c,lon}$ . The stepsize of the decay is a function of  $\tilde{\tau}_{c,o}^{-1}$  as well as of the velocities, with smaller/larger velocity differences leading to a larger/smaller drop in the survival function because of a larger/smaller time span that the ego-vehicle is subject to the distance-based risk. The different curves in fig. (3) show this effect, for a selected range of velocities.

For a pointwise approximation of the distance-based risk (no vehicle dimensions considered,  $d_{c,lon,min} = 0$ ) and large  $\beta_{c,lon}$ , the survival function approaches a step function with a step at the time of closest encounter  $s_c$  from (20) and a velocity-independent step size  $\gamma$ ,

$$S(t+s; t, \mathbf{z}_{t:t+s}) \approx 1 - \gamma \Theta[s - s_c(v^o, x^i, v^i)] \quad (24)$$

The accumulated event probability then reduces to

$$A_{\text{event}}(t+s; t, \mathbf{z}_{t:t+s}) \approx \gamma \Theta[s - s_c(v^o, x^i, v^i)] \quad (25)$$

which is used to calculate the average number of collision accidents, resulting as a consequence of passing maneuvers.

### C. Collision Accident Rates as Function of Vehicle Velocity

From now on, we do not consider single other vehicles but a **continuum**, so that we omit the indices  $i$ , use  $x$  and  $v$  for the other cars' position and velocity, and write e.g. for the one-dimensional spatial vehicle density of other cars at time 0

$$\rho(x) = \sum_{i=1}^N \delta(x - x^i) \quad (26)$$

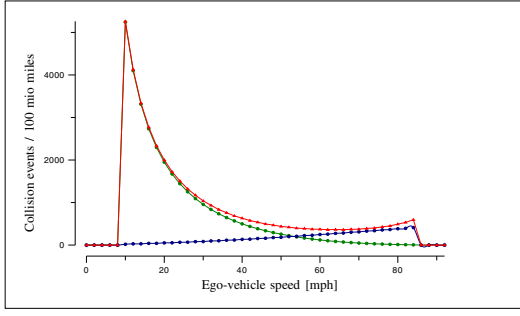


Fig. 4. Contributions of passing (blue) and being passed (green) to the calculation of the total number of collision events (red), as a function of ego-vehicle speed  $v^o$ . As expected, the number of passing / being passed vehicles decreases / increases with an increase of speed.

so that

$$\int_{-\infty}^{\infty} \rho(x) dx = N \quad (27)$$

For the case of steady traffic flow and therefore stationary and homogeneous traffic density  $\rho(x)$  (number of cars per longitudinal distance) as well as stationary velocity distribution  $p(v)$ , we then get the total number of events that occur during a time interval of length  $s$  by integrating (25) according to

$$\begin{aligned} N_{\text{events}}(s, v^o) &= \quad (28) \\ &= \int_{-\infty}^{+\infty} p(v) \int_{-\infty}^{+\infty} \rho(x) A_{\text{event}}(s; 0, \mathbf{z}_{o;s}) dx dv \\ &= \gamma \int_{-\infty}^{+\infty} p(v) \int_{-\infty}^{+\infty} \rho(x) \Theta[s - s_c(v^o, x, v)] dx dv . \end{aligned}$$

In this case, the main cause of risk and thus, of accident events, is given by the number of passing encounters. That is, the number of accidents is roughly proportional to the number of times that a vehicle passes other vehicles or that it is passed from behind.

For the calculation of  $N_{\text{events}}(s, v^o)$ , we fix an observation time interval of length  $s$  and accumulate the risk of each passing maneuver. Another vehicle, located at  $x$  and driving with  $v$ , will pass the ego vehicle if

- either it is in front of the ego vehicle and has a velocity which is so much lower than  $v^o$  that it will be passed by the ego-vehicle during  $s$ , which happens when  $x \leq (v^o - v)s$ ,
- or it is at the back of the ego vehicle and has a velocity which is so much faster than  $v^o$  that it will pass the ego vehicle during  $s$ , which happens when  $x \geq (v^o - v)s$ .

Inserting these conditions  $x \leq (v^o - v)s$  into (28), we get the number of collision events from flow equations (compare [2]) which contain the survival probability step parameter  $\gamma$ ,

$$\begin{aligned} N_{\text{events}}(s, v^o) &= \gamma \int_{-\infty}^{v^o} p(v) \int_{x^o}^{x^o + (v^o - v)s} \rho(x) dx dv \\ &+ \gamma \int_{v^o}^{+\infty} p(v) \int_{x^o + (v^o - v)s}^{x^o} \rho(x) dx dv . \quad (29) \end{aligned}$$

With constant traffic density (as e.g. given during stationary flow conditions)  $\rho(x) := \rho$  we can reduce the spatial integral

to get

$$\begin{aligned} N_{\text{events}}(s, v^o) &= \underbrace{\gamma \rho s \int_{-\infty}^{v^o} p(v) (v^o - v) dv}_{\text{Ego vehicle passes}} \\ &+ \underbrace{\gamma \rho s \int_{v^o}^{+\infty} p(v) (v - v^o) dv}_{\text{Ego vehicle being passed}} , \quad (30) \end{aligned}$$

with both terms being strictly positive and denoting the probabilities for the different passing conditions.

#### D. Collision Accident Rates for Deviations from Average Velocity

In the following, it is assumed that for the ego vehicle we look at positive and negative variations starting from a reference velocity  $\hat{v}$ , that is, we consider the ego vehicle to be driving faster or slower than  $\hat{v}$  so that  $v^o = \hat{v} \pm \Delta v^o$ . With some substitutions, we get

$$\begin{aligned} N_{\text{events}}(s, \hat{v}, \pm \Delta v^o) &= \quad (31) \\ &= \gamma \rho s \int_0^{+\infty} [p(-v + \hat{v} \pm \Delta v^o) + p(v + \hat{v} \pm \Delta v^o)] v dv . \end{aligned}$$

Eq. (31) is the compact form of the expected number of collision accidents under the given assumptions, and can be used for any velocity distribution  $p(v)$ .

From statistical measurements in normal driving environments like roads without many intersections, the velocity distribution can be extracted. This distribution often resembles a Gaussian  $g_{\bar{v}, \sigma}$  with mean  $\bar{v}$  and standard deviation  $\sigma$ , so let us consider this as a good representative parameterization of  $p(v)$  and  $p(v) = g_{\bar{v}, \sigma}(v)$ .

A Gaussian distribution is symmetric around the mean, so that  $g_{\bar{v}, \sigma}(\bar{v} \pm \Delta v) = g_{\bar{v}, \sigma}(\bar{v} \mp \Delta v)$ . In this case, if we take the reference velocity from above to be at the Gaussian mean ( $\hat{v} = \bar{v}$ ), we get

$$\begin{aligned} N_{\text{events}}(s, \bar{v}, \pm \Delta v^o) &= \quad (32) \\ &= \gamma \rho s \int_0^{+\infty} [g_{\bar{v}, \sigma}(-v + \bar{v} \pm \Delta v^o) + g_{\bar{v}, \sigma}(v + \bar{v} \pm \Delta v^o)] v dv \\ &= \gamma \rho s \int_0^{+\infty} [g_{o, \sigma}(v \mp \Delta v^o) + g_{o, \sigma}(v \pm \Delta v^o)] v dv \end{aligned}$$

The same considerations apply for any symmetric distribution. This means that, for a symmetric velocity distribution, the number of expected accidents during a fixed time interval is also symmetric for variations  $\pm \Delta v^o$  around its mean velocity  $\bar{v}$ . For non-zero  $\pm \Delta v^o$ , the accident numbers increase symmetrically for both lower as well as higher velocities. That is, the number of accidents is lowest if we “**drive with the flow**”, and increases when we deviate from it in either direction. It does not make any difference (in terms of number of accidents) if we drive faster or slower than the average velocity.

The symmetry is broken for the accident risk, which is a combination of the probability that an accident happens with the accident severity, since the severity always increases for greater speeds. The influence of this effect for small ranges of  $\pm \Delta v^o$  around  $\bar{v}$  does however not have a large influence, as already noted [2].

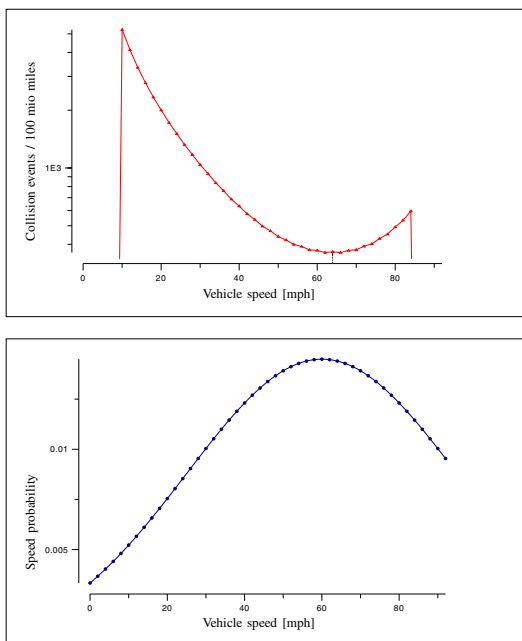


Fig. 5. Top: The Solomon curve as calculated from the number of expected collision events using a spatial risk model based on survival risk theory for passing and being passed. Note the minimum at speeds slightly above 60 mph, indicated by a vertical black line. Compare with fig. 1. Bottom: Assumed velocity distribution with mean at 60 mph.

## V. RELATION TO THE SOLOMON-CURVE

What we have calculated is the expected number of accidents during a time interval. It is often more convenient to suppress the time interval  $s$ ,

$$n_{\text{events}} := N_{\text{events}}(s, v^o)/s \quad (33)$$

for which we get from (32)

$$n_{\text{events}}(\bar{v}, \pm \Delta v^o) = \gamma \rho \int_0^{+\infty} [g_{o,\sigma}(v \mp \Delta v^o) + g_{o,\sigma}(v \pm \Delta v^o)] v dv \quad (34)$$

which is the temporal accident **rate**, that is, the number of accidents per time unit.

Instead of the number of accidents per time unit, we now consider  $\bar{n}_{\text{events}}$ , the number of accidents per traveled distance. The traveled distance during the time interval  $s$  for the ego vehicle with velocity  $v^o$  is  $v^o s$ . The absolute number of accidents during that time interval is then  $\bar{n}_{\text{events}} v^o s$  and it holds

$$\bar{n}_{\text{events}} v^o s = n_{\text{events}} s \quad (35)$$

so that we finally arrive at

$$\bar{n}_{\text{events}} = n_{\text{events}}/v^o. \quad (36)$$

This means that the number of accidents **per traveled distance** is calculated by dividing the (temporal) accident rate by the ego vehicle velocity, which causes the curve to be asymmetrically skewed with a minimum at velocities larger than the mean velocity  $\bar{v}$ .

Figure 5 top shows  $\bar{n}_{\text{events}}$  calculated using (36) and (34), with the dimensions of number of accidents per 100 million

traveled miles, as a log-plot which can be compared directly with the original Solomon curve. Below, we show the speed distribution used for the calculation, which has its mean at 60 mph. We used a constant (i.e., velocity-independent)  $\gamma$ ,  $\gamma \rho = 1100$ , velocity mean  $\bar{v} = 60$  and standard deviation  $\sigma = 15$  mph.

## VI. DISCUSSION

From comparing figs. 1 and 5, one can see that the quantitative dependency of the Solomon curve can be reproduced almost perfectly by our model. The only remaining free parameters are  $\gamma$  and  $\rho$ , which can be adapted to model conditions like heavy traffic, weather and night time. Since  $\rho$  is the longitudinal vehicle density (number of vehicles on a road section divided by the road section length), this can be easily measured, so that the remaining parameter is  $\gamma$ , the amount of decrease of the survival probability when two cars pass each other.

This means that knowing  $\rho$  and Solomon-curve-type measurement data of collision events, by fitting the experimental with the theoretical curve we can get an estimate for  $\gamma$ . Based on that, we can also get an estimate for the microscopical spatial risk parameters  $\tilde{\tau}_{c,o}^{-1}$  and  $\beta_{c,lon}$  from (23), which would indeed be very interesting because such a validated microscopic risk model could then (i) be used to predict risk statistics for other driving situations or (ii) to apply the model on single situations giving warnings about the current risk rate during driving. In particular, it could be used in dedicated microscopic risk modeling of traffic situations as analyzed in [7], [8], [9], and extensions.

As explained in section V, although the number of collisions per time  $n_{\text{events}}$  is symmetric around the mean speed  $\bar{v}$ , the number of collisions per traveled distance  $\bar{n}_{\text{events}}$  is not. This is because during for the same accumulated risk during a time interval, at higher speeds, a larger traveled distance is covered. In fig. 5, the consequence can be clearly seen in form of a U-shaped curve that has a minimum which is not exactly at  $\bar{v}$ , but at slightly higher velocities.

It has been argued previously that the origin of this asymmetry might be a consequence of a non-symmetric velocity distribution, either because in reality it is not Gaussian or because the distribution might be multimodal, e.g. with further peaks either at the very low or the very high speed range. We investigated this by numerical simulations but could not confirm this assumption, so that the most likely explanation seems to be the one presented in section V. However, for the analytic calculations from section V, as an approximation, we have used the assumption that  $\gamma$  is constant, whereas it can be clearly seen from fig. 3 that  $\gamma$  decreases monotonously with higher velocities. This leads to a modification of the calculation of the number of collision

events so that (30) has to be modified to

$$N_{\text{events}}(s, v^o) = \underbrace{\rho s \int_{-\infty}^{v^o} \gamma(v) p(v) (v^o - v) dv}_{\text{Ego vehicle passes}} + \underbrace{\rho s \int_{v^o}^{+\infty} \gamma(v) p(v) (v - v^o) dv}_{\text{Ego vehicle being passed}} .$$

A numerical evaluation of this effect revealed that this shifts the minimum of the Solomon curve to even higher velocities. With more empirical data available, it would be interesting to explore to which extent additional shifts of the minimum of the Solomon curve w.r.t. the maximum of the speed distribution can be attributed to this effect.

The theoretical derivation according to (36) and (34) provides a close fit to the Solomon curve from very low speeds up to speeds closely above the average  $\bar{v}$ . For higher speeds  $v^o$ , the effect of the division by  $v^o$  in  $\bar{n}_{\text{events}} = n_{\text{events}}/v^o$  reduces the increase of the curve at the right side of the U-shape. In fact, at high speeds  $v^o \gg \bar{v}$  the collision rates of the Solomon curve increase faster than theoretically derived. We plan to investigate this in future work, but it seems that an additional velocity-dependent risk contribution will be needed which accounts for higher collision involvement rates at very high speeds, e.g. by considering reduced physical controllability or larger consequences of driving errors at high speeds.

A full risk consideration would take, in addition to the probability that an event might happen, the respective **severity** of the accidents into account. At high speed differences, the probability of severe accidents rises sharply, implying larger risks. However, around the minimum of the U-shaped Solomon curve, this effect is not dominant (as argued originally by [2]). Even for the full risk including severity considerations, it is therefore safer to **drive with the flow** with velocities  $v^o \approx \bar{v}$  because at this speed the number of dangerous passing events reaches its minimum.

The Solomon curve as well as our theoretical derivations suggest that one should drive even slightly faster than the average, as can be observed by the shifted minimum in figs. 1 and 5 for  $\bar{n}_{\text{events}}$  (the **number of accidents per travelled distance**). This is somewhat paradoxical, since for  $n_{\text{events}}$  (the **number of accidents per time**) the minimum is still at  $\bar{v}$ , suggesting that one should drive exactly with the flow. Looking closely, we see that  $\bar{n}_{\text{events}}$  does not account for risk per se (resp. occurrence probability), but for a mixture of risk combined with traveling efficiency. Being exposed to dangerous situations for longer times bears a higher risk, so that it is beneficial to keep these time periods as short as possible. In terms of risk, it is sometimes preferable to trade higher velocities (which imply higher severity in case that something happens) for lower times being exposed to risk (reducing the chance that something happens). To understand this effect, think of passing a strangely wobbling truck in front of you, where it is favorable to keep the passing maneuver short with a high velocity difference as compared to passing

with a very low differential speed, but staying beside the truck for a long time period.

The fact that the Solomon curve can be almost perfectly explained with the passing model does by no means imply that the only risks during driving in similar conditions are accounted for by passing events. One could certainly ask about the risk of more complicated maneuvers like lane changes, overtaking, entrance and exit maneuvers, etc., with each of them probably bearing a **higher risk per situation** than passing maneuvers. The point is, that the overall frequency of these maneuvers is usually much lower so that the statistics are still dominated by passing events. Nevertheless, once we have a good validation of the risk model parameters as proposed in this work, we can apply the microscopic risk model to these or arbitrary other maneuvers as well.

## ACKNOWLEDGMENT

The author would like to thank Stefan Klingelschmitt, Florian Damerow and Benedict Flade for their valuable discussions and comments which helped to improve the manuscript.

## REFERENCES

- [1] D. Solomon, "Accidents on main rural highways related to speed, driver, and vehicle," U.S. Department of Commerce/Bureau of Public Roads (precursor to Fed. Highway Administration), Tech. Rep., 1964.
- [2] E. Hauer, "Accidents, overtaking and speed control," *Accident Analysis & Prevention*, 1971.
- [3] Volvo, "Volvo drive me announcement," 2013, [Online; accessed 10-May-2016]. [Online]. Available: <https://www.media.volvocars.com/global/en-gb/media/pressreleases/136182/volvo-car-group-initiates-world-unique-swedish-pilot-project-with-self-driving-cars-on-public-roads>
- [4] H. Lum and J. A. Reagan, "Interactive highway safety design model: Accident predictive module," *Public Roads Magazine*, 1995.
- [5] E. Rendon-Velez, "Recognizing driving in haste," Ph.D. dissertation, TU Delft, 2014.
- [6] J. Eggert, "Predictive risk estimation for intelligent adas functions," in *Intelligent Transportation Systems (ITSC)*. IEEE, 2014, pp. 711–718.
- [7] J. Eggert and F. Damerow, "Complex lane change behavior in the foresighted driver model," in *Intelligent Transportation Systems (ITSC)*. IEEE, 2015.
- [8] J. Eggert, B. Flade, and F. Damerow, "Extensions for the foresighted driver model: Tactical lane change, overtaking and continuous lateral control," in *Intelligent Vehicles Symposium (IV)*. IEEE, 2016.
- [9] J. Eggert, S. Klingelschmitt, and F. Damerow, "The foresighted driver: Future adas based on generalized predictive risk estimation."
- [10] G. P. C.N. Kloeden and A. McLean, "Travelling speed and the risk of crash involvement on rural roads," Adelaide University, Tech. Rep., 2001.
- [11] J. Cirillo, "Interstate system accident research study ii, interim report ii," *Public Roads*, 1968.
- [12] S. L. Johnson and N. Pawar, "Cost-benefit evaluation of large truck-automobile speed limit differentials on rural interstate highways," University of Arkansas, Department of Industrial Engineering, Tech. Rep., 2005.
- [13] , "Speed and accident, volume ii, report no. fh-11-6965," Research Triangle Institute, National Highway Safety Bureau, Tech. Rep., 1970.
- [14] N. C. D. J. R. A. W. E. B. R. L. Monsere, C. M. and C. Milliken, "Impacts and issues related to proposed changes in oregons interstate speed limits," Portland State University, Tech. Rep., 2004.
- [15] J. West, L. B. and J. W. Dunn, "Accidents, speed deviation and speed limits," *Traffic Engineering*, 1971.
- [16] Wikipedia, "Risk — Wikipedia, the free encyclopedia," 2014, [Online; accessed 12-May-2014]. [Online]. Available: <http://en.wikipedia.org/w/index.php?title=Risk&oldid=608166233>
- [17] S. N. Luko, "Risk management - Principles and Guidelines," *Quality Engineering*, vol. 25, no. 4, pp. 451–454, 2009.